

area (CD68), cells per unit area (CD4, PCNA) or percent of total plaque area (CD31, alpha-SM actin, CD11c, CD83, VCAM-1, MCP-1).<sup>10</sup>

### **mAbs and Flow Cytometry**

The following antibodies were used: anti-CD4-pacific blue (BD Pharmingen), anti-CD8-PerCP (BD Pharmingen), anti-TCR $\beta$ -APC (Pharmingen), anti-NK1.1-PE Cy7 (Pharmingen), anti-CD25-APC Cy7 (Pharmingen), Foxp3-PE (BD Pharmingen), anti-CD11c-PE (eBioScience), anti-F4/80-Alexafluor (647) eBioScience), anti-CD11b-PerCP-Cy5.5 (eBioScience) and anti-Gr1 (Ly6G and Ly6C)-AlexaFluor-488 (eBioScience).<sup>11</sup> Spleens and lymph nodes were gently dissociated between the frosted ends of glass slides to obtain single cell suspensions which were passed through a 70 $\mu$ M nylon strainer. Single cell suspensions were pre-incubated with anti-FcR $\gamma$  (2.4G2) to prevent non-specific staining followed by incubation with fluorochrome-conjugated primary antibodies for 30 minutes at 4°C. For Foxp3 staining the cells were permeabilized using the BD Pharmingen Mouse Foxp3 buffer set according to the manufacture's directions. For analyses of monocytes and dendritic cells in blood and lymph nodes the following antibodies were used: NK1.1-PE, CD22-PE, CD90-PE, CD49b-PE, Ly-6G-PE, CD11b-APC-Cy7, Ly-6C-pacific blue, CD11c-APC and BrdU-PerCP (all from BD Pharmingen), I-A<sup>b</sup>-PE-Cy7 (BioLegend) and CD115-Alexa-488 (eBiosciences). Monocytes in blood were identified as CD11b<sup>hi</sup>CD90<sup>lo</sup>CD22<sup>lo</sup>CD49b<sup>lo</sup>NK1.1<sup>lo</sup>Ly-6G<sup>lo</sup> and monocyte-derived dendritic cells as CD11c<sup>hi</sup>CD11b<sup>hi</sup>CD90<sup>lo</sup>CD22<sup>lo</sup>CD49b<sup>lo</sup>NK1.1<sup>lo</sup>Ly-6G<sup>lo</sup>.<sup>12</sup> Sample data was acquired using a BD FACS Canto II (BD Biosciences).

### **HMGB1 Elisa**

HMGB1 in plasma was measured using an ELISA HMGB1 detection kit (Apotech Corp, Enzo Life Sciences GMBH, Germany) according to the manufacture's instructions. The sensitivity of the assay is approximately 1ng/ml.

## **Macrophage Chemotaxis in Vitro and in Vivo**

Macrophage chemotaxis in vitro was measured using fibronectin-coated-8 $\mu$ m porous transwells (BD Biosciences). Briefly, RAW264.7 mouse macrophages (200,000) were cultured in DMEM containing 1% fetal calf serum prior to being loaded onto the inserts which were placed in 24-well plates containing DMEM in the presence or absence of 4 $\mu$ g/ml HMGB1 and incubated at 37°C for 15 hours. Non-migrated cells in the top chamber were removed using cotton swabs before fixing the migrated cells in methanol-glacial acetic acid (3:1) and staining with crystal violet. Chemotaxis was quantified by counting the number of migrated cells in five random high-power microscopy fields per well.<sup>13</sup> To determine whether HMGB1 induced macrophage chemotaxis in vivo mice were injected i.p. with 1ml of vehicle (0.9% NaCl) or HMGB1 (20 $\mu$ g/ml in 0.9% NaCl). After 5 hours the mice were sacrificed and the cellular contents of their intraperitoneal cavities were collected by sequential lavages in PBS. After centrifugation, red blood cells were lysed with ammonium chloride-potassium carbonate-EDTA buffer (0.15M NH<sub>4</sub>Cl, 1mM KHCO<sub>3</sub> and 0.1mM Na<sub>2</sub>EDTA in PBS) and total cell numbers determined. Then the cells were pre-incubated with anti-FcR $\gamma$  (2.4G2) to prevent non-specific staining followed by incubation with fluorochrome-conjugated primary antibodies-anti-F4/80, anti-CD11b, anti-CD11c and anti-Gr-1 (see mAbs and Flow Cytometry) for 30 minutes at 4°C. Sample data was acquired using a BD FACS Canto II (BD Biosciences).

## **Analysis of Gene Expression**

Total RNA was extracted from tissues as previously described<sup>14</sup> and resuspended in sterile water; any contaminating DNA was removed by incubating the RNA extracts with 2 U DNase (Stratagene), for 15 minutes at 37°C. Then 2  $\mu$ L of 2 mol/L sodium acetate followed by an equal volume of isopropanol was added and the precipitated RNA was sedimented by centrifugation. The RNA pellet was washed by resuspension in 70% aqueous ethanol followed by centrifugation, and then air dried for 30 minutes. This purified RNA was dissolved in sterile water and quantitated by spectrophotometry at 260 nm. The

extracted total RNA was reverse transcribed using TaqMan methodology (Applied Biosystems) as described by the manufacturer. Then 40ng of cDNA was used for real-time PCR to determine the expression of each gene using Applied Biosystems SYBR Green PCR Mix and the ABI Prism 7500 system. Each amplification was performed in duplicate and included internal controls for CD68 (macrophages) to take into account any alterations in lesion size. Relative amounts of each mRNA for each of the genes in lesions from control and anti-HMGB1 treated ApoE<sup>-/-</sup> mice were calculated using comparative C<sub>T</sub> values.<sup>4</sup> The sequences of oligonucleotides used were, TIM-1: sense, 5'-AGTGACCTTTTCATTGCAAGTTAAAC-3' and antisense, 5'-GCTGTGG GCCTTG TAGTTGTG-3'; for TIM-3: sense, 5'-CAGCTTCTCCAAGAACCCTAACC-3' and antisense, 5'-TTATTATGGAGGGTCACCAGTGTCT-3'; for IL-6: sense, 5'-GAAATGAT GGATGCTACCAAAGT-3' and antisense, 5'-CCAGAAGACCAGAGGAAATTTTCA-3'; for TNF- $\alpha$ : sense, 5'-CTATGGCCCAGACCCTCACA-3' and antisense, 5'-TCCTCCACTTG GTGGTTTGC-3'; for IFN- $\alpha$ : 5'-TCCTCAGACTCATAACCTCAGGAA-3' and antisense, 5'-GGGAGAGTCTCCTCATTTGTACCA-3'; for IL-1 $\beta$ : sense, 5'-CCACCTCAATGGACAGAA TATCAA-3' and antisense, 5'-GTCGTTGCTTGGTTCTCCTTGT-3'; for 18s: sense, 5'-CGGCTACCACATCCAAGGAAGGCA-3' and antisense, 5'-GCTGGAATTACCGCGGCTGCTGGC-3' ; for CD68: sense, 5'-TGACCTGCTCTCTCTAAGGCTACA-3 and antisense, 5'-TGGTCACGGTTGCAAGAGAA-3.

### **Statistical Analyses**

Statistical analyses were performed using Student's t-test when data followed a normal distribution or Mann-Whitney U test when data did not follow a normal distribution, using the software GraphPad Prism v4.01. P < 0.05 was considered statistically significant.

## References for Supplemental Materials and Methods

1. Liu K, Mori S, Takahashi HK, Tomono Y, Wake H, Kanke T, Sato Y, Hiraga N, Adachi N, Yoshino T, Nishibori M. Anti-high mobility group box 1 monoclonal antibody ameliorates brain infarction induced by transient ischemia in rats. *FASEB J*. 2007; 21: 3904-3916.
2. Mittler RS, Bailey TS, Klussman K, Trailsmith MD, Hoffmann MK. Anti-4-1BB monoclonal antibodies abrogate T cell-dependent humoral immune responses in vivo through the induction of helper T cell anergy. *J Exp Med*. 1999; 190: 1535-1540.
3. Vieira P, Rajewsky K. The half-lives of serum immunoglobulins in adult mice. *Eur J Immunol*. 1988; 18: 313-316.
4. Palumbo R, Sampaolesi M, De Marchis F, Tonlorenzi R, Colombetti S, Mondino A, Cossu G, Bianchi ME. Extracellular HMGB1, a signal of tissue damage, induces mesoangioblast migration and proliferation. *J Cell Biol*. 2004; 164: 441-449.
5. Muller S, Bianchi ME, Knapp S. Thermodynamics of HMGB1 interaction with duplex DNA. *Biochemistry*. 2001; 40: 10254-10261.
6. Penzo M, Molteni R, Suda T, Samaniego S, Raucci A, Habel DM, Miller F, Jiang H, Li J, Pardi R, Palumbo R, Olivetto E, Kew RR, Bianchi ME, Marcu KB. Inhibitor of NF- $\kappa$ B kinases  $\alpha$  and  $\beta$  are both essential for high mobility group Box 1-mediated chemotaxis. *J Immunol*. 2010; 184: 4497-4509.
7. Paigen B, Morrow A, Holmes PA, Mitchell D, Williams RA. Quantitative assessment of atherosclerotic lesions in mice. *Atherosclerosis* 1987; 68: 231-240.
8. Lewis P, Stefanovic N, Pete J, Calkin AC, Giunti S, Thallas-Bonke V, Jandeleit-Dahm KA, Allen TJ, Kola I, Cooper ME, de Haan JB. Lack of the antioxidant enzyme glutathione peroxidase-1 accelerates atherosclerosis in diabetic apolipoprotein E-deficient mice. *Circulation*. 2007; 115: 2178-2187.

9. To K, Agrotis A, Besra G, Bobik A, Toh BH. NKT cell subsets mediate differential proatherogenic effects in ApoE<sup>-/-</sup> mice. *Arterioscler Thromb Vasc Biol.* 2009; 29: 671-677.
10. Raj T, Kanellakis P, Pomilio G, Jennings G, Bobik A, Agrotis A. Inhibition of fibroblast growth factor receptor signaling attenuates atherosclerosis in Apolipoprotein E-deficient mice. *Arterioscler Thromb Vasc Biol.* 2006; 26: 1845-51.
11. Daley JM, Thomay AA, Connolly MD, Reichner JS, Albina JE. Use of Ly6G-specific monoclonal antibody to deplete neutrophils in mice. *J Leukocyte Biol.* 2008; 83: 64-70.
12. Swirski FK, Libby P, Aikawa E, Alcaide P, Luscinskas FW, Weissleder R, Pittet MJ. Ly-6C<sup>hi</sup> monocytes dominate hypercholesterolemia-associated monocytosis and give rise to macrophages in atheroma. *J Clin Invest.* 2007; 117: 195-205.
13. Chiou W-F, Shum A Y-C, Peng C-H, Chen C-F, Chou C-J. Piperlactam S suppresses macrophage migration by impeding F-actin polymerization and filopodia extension. *Eur J Pharmacol.* 2003; 458: 217-225.
14. Ward MR, Agrotis A, Kanellakis P; Dilley R, Jennings G, Bobik A. Inhibition of Protein Tyrosine Kinases Attenuates Increases in Expression of Transforming Growth Factor- $\beta$  Isoforms and Their Receptors Following Arterial Injury. *Arterioscler Thromb and Vasc Biol.* 1997;17:2461-2470.

## Legends for Supplementary Tables and Figures

**Table I:** Plasma Lipid Levels in ApoE<sup>-/-</sup> mice treated with control or anti-HMGB1 antibody (Ab) and fed a high fat diet for 8 weeks. Results are means  $\pm$  SEM.

**Table II.** Monocyte subtypes and dendritic cells in blood (cells/ml) and lymph nodes (cell numbers) of ApoE<sup>-/-</sup> mice treated with control or anti-HMGB1 antibody (Ab) and injected with bromodeoxyuridine (1mg, i.p.) for 3 consecutive days before culling. Results are means  $\pm$  SEM of 4 mice in each group.

**Figure I.** Immunohistochemistry of aortic sinus atherosclerotic lesions from control (left) and anti-HMGB1 neutralizing antibody (right) treated ApoE<sup>-/-</sup> mice fed a high fat diet. Cross sections were stained with anti-alpha-SM actin antibody to detect smooth muscle cells associated with lesions (top), anti-CD31 antibody to detect endothelial cells associated with lesions (middle) and anti-proliferating nuclear antigen (PCNA) antibody to detect cell proliferation (bottom). Bar graphs represent differences between the two groups. Red: control and blue: anti-HMGB1 antibody treatment. \*P < 0.05 from control. Size bars on photomicrographs represent 100 $\mu$ m.

**Figure II.** Lymphocyte populations (CD4<sup>+</sup> T cells, CD19<sup>+</sup> B cells, NK1.1<sup>+</sup> NK cells, NK1.1<sup>+</sup>TCR<sup>+</sup> NKT cells and CD4<sup>+</sup>Foxp3<sup>+</sup> regulatory T cells [Tregs]) in blood, spleen and para-aortic lymph nodes following treatment with control (open boxes) or anti-HMGB1 neutralising antibodies (shaded boxes). Bar graphs represent means  $\pm$  SEM of three mice in each group.

**Figure III.** Expression of proinflammatory mediators in atherosclerotic lesions following treatment with control (left) or anti-HMGB1 neutralizing antibodies (right). Top, photomicrographs of aortic sinus lesions stained with anti-VCAM-1 antibodies; middle:

aortic lesions stained with anti-MCP-1 antibodies and bottom real time PCR analyses of TNF- $\alpha$ , IFN- $\alpha$ , IL-6 and IL-1 $\beta$  expression in aortic atherosclerotic lesions. Bar graphs represent differences between the two groups. Red: control and blue: anti-HMGB1 antibody treatment. \*P < 0.05 from control. Size bars on photomicrographs represent 100 $\mu$ m

**Table I**

<b>Treatment</b>	<b>Total Cholesterol (mmol/l)</b>	<b>HDL-Cholesterol (mmol/l)</b>	<b>LDL-cholesterol (mmol/l)</b>	<b>Triglycerides (mmol/l)</b>
<b>Control Ab</b>	7.55 ± 0.33	1.27 ± 0.05	5.19 ± 0.22	2.46 ± 0.22
<b>HMGB1 Ab</b>	7.70 ± 0.38	1.30 ± 0.08	5.45 ± 0.29	2.14 ± 0.13



**Table II**

<b>MONOCYTE/DENDRITIC CELLS*</b>	<b>Control Ab</b>	<b>Anti-HMGB1 Ab</b>
<b>Blood</b>		
BrdU+CD11b <sup>hi</sup> Ly-6C <sup>hi</sup>	0.032 ± 0.017 × 10 <sup>6</sup>	0.044 ± 0.009 × 10 <sup>6</sup>
CD11b <sup>hi</sup> Ly-6C <sup>hi</sup>	0.103 ± 0.045 × 10 <sup>6</sup>	0.099 ± 0.024 × 10 <sup>6</sup>
CD11b <sup>hi</sup>	0.137 ± 0.056 × 10 <sup>6</sup>	0.130 ± 0.024 × 10 <sup>6</sup>
BrdU+CD11c <sup>hi</sup> CD11b <sup>hi</sup>	0.0348 ± 0.016 × 10 <sup>6</sup>	0.0394 ± 0.008 × 10 <sup>6</sup>
CD11c <sup>hi</sup> CD11b <sup>hi</sup>	0.082 ± 0.035 × 10 <sup>6</sup>	0.088 ± 0.025 × 10 <sup>6</sup>
CD11c <sup>hi</sup> CD11b <sup>hi</sup> I-A <sup>b(hi)</sup> CD115 <sup>hi</sup>	0.0097 ± 0.0048 × 10 <sup>6</sup>	0.0111 ± 0.0027 × 10 <sup>6</sup>
<b>Inguinal Lymph Nodes</b>		
CD11c <sup>hi</sup> CD11b <sup>hi</sup> I-A <sup>b(hi)</sup> CD115 <sup>hi</sup>	0.007 ± 0.003 × 10 <sup>6</sup>	0.008 ± 0.003 × 10 <sup>6</sup>
<b>Mediastinal Lymph Nodes</b>		
CD11c <sup>hi</sup> CD11b <sup>hi</sup> I-A <sup>b(hi)</sup> CD115 <sup>hi</sup>	0.0014 ± 0.004 × 10 <sup>6</sup>	0.0027 ± 0.0021 × 10 <sup>6</sup>

\* All cells are CD90<sup>lo</sup>CD49b<sup>lo</sup>NK1.1<sup>lo</sup>Ly-6G<sup>lo</sup>CD22<sup>lo</sup>

**Figure 1**

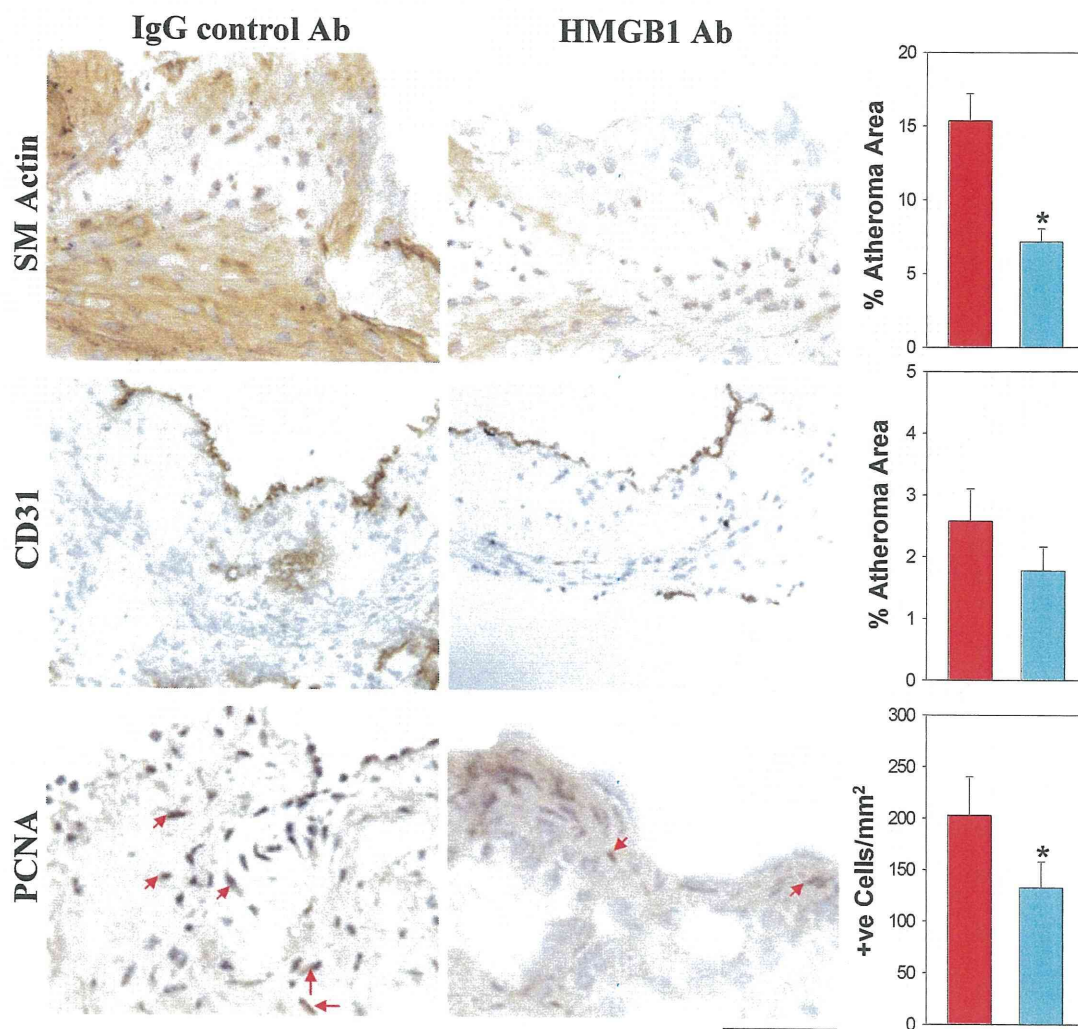


Figure II

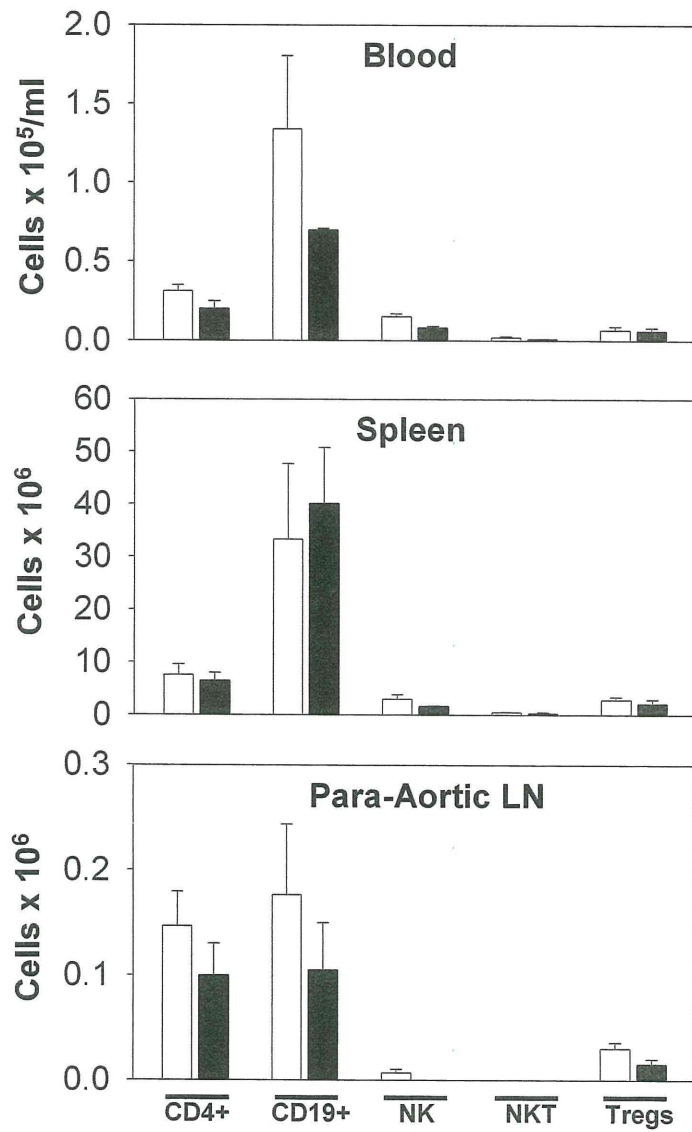
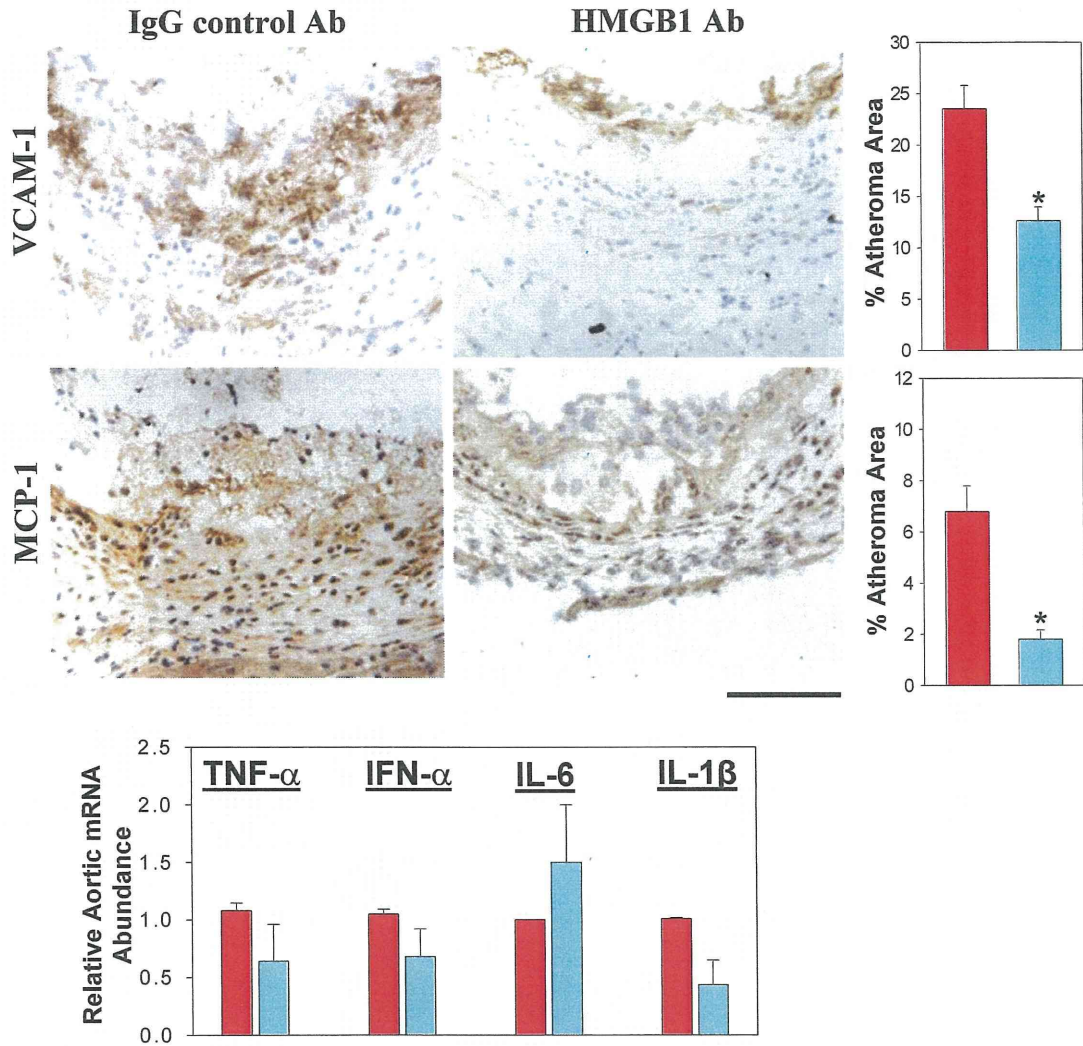
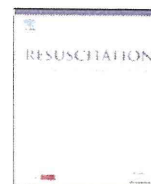


Figure III





## Experimental paper

Reduction of the infarct size by simultaneous administration of L-histidine and diphenhydramine in ischaemic rat brains<sup>☆</sup>Naoto Adachi<sup>a,\*,</sup> Keyue Liu<sup>b</sup>, Kanji Ninomiya<sup>a</sup>, Eiko Matsuoka<sup>a</sup>, Atsuko Motoki<sup>c</sup>, Yumi Irisawa<sup>d</sup>, Masahiro Nishibori<sup>b</sup><sup>a</sup> Mabuchi Clinic, Kyoto-shi, Kyoto, Japan<sup>b</sup> Department of Pharmacology, Okayama University Graduate School of Medicine, Dentistry and Pharmaceutical Sciences, Okayama-shi, Okayama, Japan<sup>c</sup> Department of Anesthesia, Japanese Red Cross Kyoto Daini Hospital, Kyoto-shi, Kyoto, Japan<sup>d</sup> Department of Anesthesia, Noto General Hospital, Nanao-shi, Ishikawa, Japan

## ARTICLE INFO

## Article history:

Received 2 July 2010

Received in revised form 20 August 2010

Accepted 20 October 2010

## Keywords:

Brain ischaemia

Drug therapy

Inflammatory response

Neurons

Reperfusion

Stroke

## ABSTRACT

**Aims:** While diphenhydramine is a histamine H<sub>1</sub> receptor antagonist, the agent has been shown to inhibit histamine-*N*-methyltransferase, a histamine inactivating enzyme in the brain. Since an increase in the brain concentration of histamine ameliorates reperfusion injury after cerebral ischaemia, effects of postischaemic administration of diphenhydramine were evaluated in rats treated with L-histidine, a precursor of histamine.

**Methods:** The right middle cerebral artery was occluded for 2 h, and the infarct size was determined 24 h after reperfusion of cerebral blood flow. Brain oedema was evaluated by comparing the area of the right hemisphere to that of the left hemisphere.

**Results:** Focal cerebral ischaemia provoked marked damage in saline-treated control rats, and infarct volumes in the striatum and cerebral cortex were 56 (49–63) mm<sup>3</sup> and 110 (72–148) mm<sup>3</sup>, respectively (means and 95% confidence intervals, *n* = 6). Administration of L-histidine (1000 mg/kg, intraperitoneal) immediately after reperfusion did not affect the infarct size. Simultaneous administration of diphenhydramine (20 mg/kg, intraperitoneal) with L-histidine reduced the infarct size to 25% and 21% of that in the control group, respectively. The combination therapy completely reduced ischaemia-induced brain oedema.

**Conclusion:** Because histamine H<sub>1</sub> action does not influence ischaemic brain damage, elevation of the central histamine concentration by blockade of histamine-*N*-methyltransferase may be a likely mechanism responsible for the alleviation.

© 2010 Elsevier Ireland Ltd. All rights reserved.

## 1. Introduction

We have shown that an increase in the histamine concentration in the brain alleviates reperfusion injury after brain ischaemia by reducing inflammatory responses through histamine H<sub>2</sub> receptors.<sup>1–4</sup> Although a single dose of L-histidine (1000 mg/kg), a precursor of brain histamine, failed to improve the outcome, simultaneous administration of metoprine, a competitive inhibitor of histamine-*N*-methyltransferase, an inactivating enzyme of brain histamine, reduced the size of brain infarction.<sup>3</sup>

There are several compounds that inhibit histamine-*N*-methyltransferase activity, such as amodiaquine, tacrine, chlorpromazine and vecuronium. However, adverse effects of these agents are problematic as well as those of metoprine. Diphenhydramine, a histamine H<sub>1</sub> receptor antagonist, is usually applied to various allergic diseases and has an inhibitory effect on histamine-*N*-methyltransferase.<sup>5,6</sup> Because the agent readily passes the blood–brain barrier, and no serious adverse effect has been reported, we investigated the effect of concomitant administration of diphenhydramine and L-histidine on ischaemic brain damage.

## 2. Methods

This study was approved by the Committee on Animal Experimentation at Okayama University Graduate School of Medicine, Dentistry and Pharmaceutical Sciences, Okayama, Japan. All animals received humane care in compliance with the Principles of Laboratory Animal Care formulated by Okayama Univer-

<sup>☆</sup> A Spanish translated version of the abstract of this article appears as Appendix in the online version at doi:10.1016/j.resuscitation.2010.10.024.

\* Corresponding author at: Mabuchi Clinic, Kakimoto-cho 590-4, Shimogyo-ku, Kyoto-shi, Kyoto 600-8357, Japan. Fax: +81 75 813 3810.

E-mail address: [nadachi@mehime-u.ac.jp](mailto:nadachi@mehime-u.ac.jp) (N. Adachi).



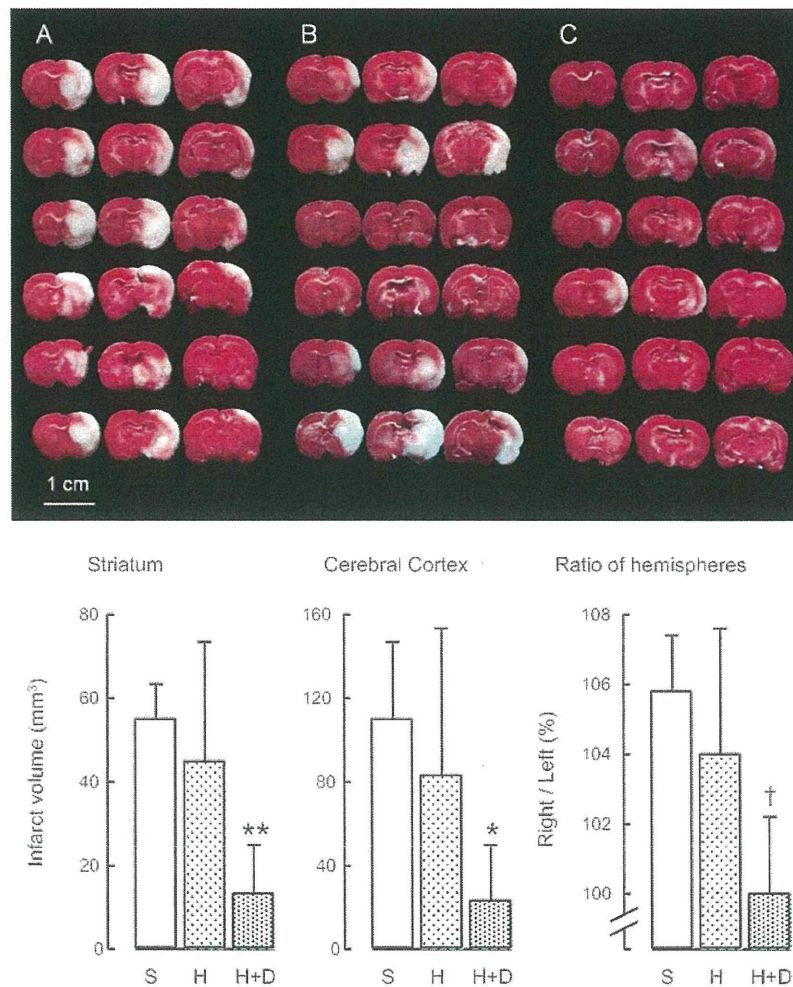


**Fig. 1.** Effects of postischemic administration of L-histidine and diphenhydramine. The right middle cerebral artery was occluded for 2 h, and L-histidine (1000 mg/kg) and diphenhydramine (20 mg/kg) were intraperitoneally administered immediately after reperfusion of cerebral blood flow. The effect was evaluated by assessing the size of brain infarction 24 h after reperfusion with 2,3,5-triphenyltetrazolium chloride stain, which turns the viable tissue a deep red colour. All brain slices in the saline-injected control (A), L-histidine (B) and L-histidine plus diphenhydramine groups (C) are shown. The size of brain infarction was measured in the striatum and cerebral cortex. Using these brain slices, the percentage of the area of the right (ischaemic) hemisphere to that of the left (non-ischaemic) hemisphere was calculated as a measure of brain oedema. Values represent means and 95% confidence intervals ( $n=6$  each). \* $p=0.02$ , \*\* $p=0.004$ , † $p=0.006$  as compared with the control group. S, saline; H, L-histidine; D, diphenhydramine.

sity Graduate School of Medicine, Dentistry and Pharmaceutical Sciences. Male Wistar rats (Charles River, Yokohama, Japan) weighing 280–300 g were kept in groups in a room controlled at  $23 \pm 2$  °C and maintained under an alternating 12-h light and 12-h dark cycle.

Eighteen rats were divided into three groups ( $n=6$  in each); the saline-injected control group, the L-histidine-injected group and the L-histidine plus diphenhydramine-injected group. The animal was anaesthetised with 2% halothane in balanced 50% oxygen and 50% nitrous oxide, and kept under spontaneous ventilation. With the rat in the supine position, the right common carotid artery was exposed, and a thermocouple needle probe was inserted into the temporal muscle to maintain the brain temperature. After an intraperitoneal injection of heparin (100 units), the root of the right middle cerebral artery was occluded by insertion of a silicone-coated 4.0 nylon thread from the bifurcation of the internal and external carotid arteries. The tip of the thread was placed 18 mm distal from the bifurcation. After the surgical incision was sutured, the animal was allowed to recover from anaesthesia. During surgery, the temperature of the temporal muscle was maintained at  $37.0 \pm 0.1$  °C with a heating lamp. All rats showed paralysis of the contralateral limbs after recovery from anaesthesia. The ani-

mal was anaesthetised again 5 min before reperfusion of the blood flow, and the skin was reopened. Cerebral blood flow was resumed 2 h after middle cerebral artery occlusion by pulling the thread by 5 mm. Then, the animal was intraperitoneally injected with saline, L-histidine (1000 mg/kg) or L-histidine (1000 mg/kg) plus diphenhydramine (20 mg/kg). The surgical incision was sutured, and the animal was allowed to recover from anaesthesia.

The animal that underwent 24 h of reperfusion was anaesthetised with an intraperitoneal injection of sodium pentobarbital, and the brain was perfused with saline. Brain slices, 2-mm thick, between the coronal planes at the optic chiasma and caudal edge of the mammillary body were incubated for 30 min with 2% 2,3,5-triphenyltetrazolium chloride in 0.1 mol/L phosphate buffer (pH 7.4) at 37 °C. 2,3,5-Triphenyltetrazolium chloride is reduced by dehydrogenase enzymes, which exist in viable cells and result in a formazan precipitate, thereby turning the tissue a deep red colour. In contrast, nonviable cells in the infarcted area show a pale gray colour with the procedure. The infarct size in the striatum and cerebral cortex was then determined, using computer-aided planimetry by an investigator who was unaware of the particular treatment group. Using these brain slices, the ratio of the area of the right

hemisphere to that of the left hemisphere was obtained in each slice. Then, the average percentage of three slices was calculated in each animal.

The data were evaluated by Scheffé's tests, and *p* values less than 0.05 were considered statistically significant.

### 3. Results

Focal cerebral ischaemia for 2 h provoked marked damage in the striatum and surrounding cerebral cortex in saline-treated control animals (Fig. 1). The infarct volumes in the striatum and cerebral cortex were 56 (49–63) mm<sup>3</sup> and 110 (72–148) mm<sup>3</sup>, respectively (means and 95% confidence intervals, *n*=6). Postischaemic administration of L-histidine (1000 mg/kg) affected the infarct size in neither the striatum (*p*=0.64) nor the cerebral cortex (*p*=0.65). Simultaneous administration of diphenhydramine (20 mg/kg) with L-histidine reduced the infarct volume in both the striatum (*p*=0.004) and cerebral cortex (*p*=0.02), and the values were 25% and 21% of those in control animals, respectively.

The ratio of the area of the right hemisphere to that of the left hemisphere was 105.8% (104.0–107.6%) in the control group. Although a single dose of L-histidine did not affect the ratio (*p*=0.54), simultaneous administration significantly reduced it (*p*=0.006).

### 4. Discussion

In the present study, L-histidine administration did not ameliorate the size of brain infarction. The finding is consistent with our previous reports that L-histidine provides no benefits at any doses by a single dose after reperfusion.<sup>3,7</sup> Simultaneous administration of diphenhydramine reduced the size of brain infarction, and the magnitude of the decrease is similar to that obtained from combination therapy with L-histidine and metoprine.<sup>3</sup> The treatment with L-histidine and diphenhydramine markedly reduced ischaemia-induced brain oedema as well as the infarct size.

In our previous study, brain infarction produced by occlusion of the middle cerebral artery for 2 h was alleviated by postischaemic administration of L-histidine (1000 mg/kg × 2), immediately and 6 h after reperfusion.<sup>2</sup> The beneficial effect was completely abolished by topical administration of ranitidine, a histamine H<sub>2</sub> receptor antagonist, indicating that an increase in the histamine level contributes to the improvement through histamine H<sub>2</sub> receptors. Considering that diphenhydramine is a potent H<sub>1</sub> antagonist and has negligible affinity for histamine H<sub>2</sub> receptors, it is unlikely that the improvement of the outcome by diphenhydramine attributes to its blocking action on histamine H<sub>1</sub> receptors.

Methylation by the specific enzyme, histamine-N-methyltransferase, is the predominant pathway of histamine inactivation in the brain, and no high-affinity uptake for histamine has been reported in brain slices, homogenates and

cultured neurones.<sup>8–10</sup> In a study on purified histamine-N-methyltransferase from the mouse brain, diphenhydramine showed a biphasic effect on histamine-N-methyltransferase activity.<sup>5</sup> At histamine concentrations below 10 μmol/L, diphenhydramine inhibited the enzyme activity. On the other hand, the agent markedly augmented it at histamine concentrations in excess of 10 μmol/L. Although the extracellular concentration of histamine increases in ischaemic brains, the concentration does not attain 10 μmol/L.<sup>7,11</sup> Therefore, diphenhydramine may show an inhibitory action on histamine-N-methyltransferase in cerebral ischaemia. Facilitation of the brain concentration of histamine by simultaneous administration may provide benefits by suppressing inflammatory responses during reperfusion through histamine H<sub>2</sub> receptors.

### 5. Conclusion

Since both L-histidine and diphenhydramine are readily transported to the brain across the blood–brain barrier, simultaneous administration of these compounds may be a new strategy for stroke.

### Conflict of interest

N. Adachi, K. Liu, A. Motoki and M. Nishibori are concerned with patent applications/registrations related to reperfusion therapies with L-histidine. K. Ninomiya, E. Matsuoka and Y. Irisawa have no conflicts of interest.

### References

- Adachi N. Cerebral ischemia and brain histamine. *Brain Res Rev* 2005;50:275–86.
- Adachi N, Liu K, Arai T. Prevention of brain infarction by postischemic administration of histidine in rats. *Brain Res* 2005;1039:220–3.
- Motoki A, Adachi N, Semba K, Liu K, Arai T. Reduction in brain infarction by augmentation of central histaminergic activity in rats. *Brain Res* 2005;1066:172–8.
- Hiraga N, Adachi N, Liu K, Nagaro T, Arai T. Suppression of inflammatory cell recruitment by histamine receptor stimulation in ischemic rat brains. *Eur J Pharmacol* 2007;557:236–44.
- Taylor KM, Snyder SH. Histamine methyltransferase: inhibition and potentiation by antihistamines. *Mol Pharmacol* 1972;8:300–10.
- Pollard S, Bischoff S, Schwartz JC. Modifications of brain HA metabolism induced by antihistamines. *Agents Actions* 1973;3:190–1.
- Irisawa Y, Adachi N, Liu K, Arai T, Nagaro T. Alleviation of ischemia-induced brain edema by activation of the central histaminergic system in rats. *J Pharmacol Sci* 2008;108:112–23.
- Hösli E, Hösli L. Autoradiographic localization of binding sites for [<sup>3</sup>H]histamine and H<sub>1</sub>- and H<sub>2</sub>-antagonists on cultured neurons and glial cells. *Neuroscience* 1984;13:863–70.
- Schayer RW, Reilly MA. Metabolism of <sup>14</sup>C-histamine in brain. *J Pharmacol Exp Ther* 1973;187:34–9.
- Schwartz JC, Pollard H, Bischoff S, Rehault MC, Verdier-Sahuque M. Catabolism of <sup>3</sup>H-histamine in the rat brain after intracisternal administration. *Eur J Pharmacol* 1971;16:326–35.
- Adachi N, Itoh Y, Oishi R, Saeki K. Direct evidence for increased continuous histamine release in the striatum of conscious freely moving rats produced by middle cerebral artery occlusion. *J Cereb Blood Flow Metab* 1992;12:477–83.



## Gene Expression and Localization of High-mobility Group Box Chromosomal Protein-1 (HMGB-1) in Human Osteoarthritic Cartilage

Chuji Terada<sup>a</sup>, Aki Yoshida<sup>a</sup>, Yoshihisa Nasu<sup>a</sup>, Shuji Mori<sup>b</sup>,  
Yasuko Tomono<sup>c</sup>, Masato Tanaka<sup>a</sup>, Hideo K. Takahashi<sup>b</sup>, Masahiro Nishibori<sup>b</sup>,  
Toshifumi Ozaki<sup>a</sup>, and Keiichiro Nishida<sup>a,d,\*</sup>

Departments of <sup>a</sup>Orthopaedic Surgery, <sup>b</sup>Pharmacology, and <sup>d</sup>Human Morphology, Okayama University Graduate School of Medicine, Dentistry and Pharmaceutical Sciences, Okayama 700-8558, Japan, and <sup>c</sup>Shigei Medical Research Institute, Okayama 701-0202, Japan

We investigated the expression and localization of high-mobility group box chromosomal protein-1 (HMGB-1) in human osteoarthritic (OA) cartilage in relation to the histopathological grade of cartilage destruction, and examined the role of HMGB-1 in the regulation of proinflammatory cytokine expression in chondrocytes. An immunohistochemical study demonstrated that total HMGB-1-positive cell ratios increase as the Osteoarthritis Research Society International (OARSI) histological grade increased. The population of cytoplasmic HMGB-1-positive chondrocytes was especially increased in the deep layers of higher-grade cartilage. The ratios and localization of receptors for advanced glycation end products (RAGE) expression by chondrocytes in Grade 2, 3, and 4 were significantly higher than those in Grade 1. *In vitro* stimulation with IL-1 $\beta$ , but not TNF $\alpha$ , significantly upregulated the expression of HMGB-1 mRNA by human OA chondrocytes. Both IL-1 $\beta$  and TNF $\alpha$  promoted the translocation of HMGB-1 from nuclei to cytoplasm. IL-1 $\beta$  and TNF $\alpha$  secretions were stimulated at higher levels of HMGB-1. The results of our study suggest the involvement of HMGB-1 in the pathogenesis of cartilage destruction in OA.

**Key words:** HMGB-1, RAGE, chondrocyte, osteoarthritis, cartilage

Osteoarthritis (OA) is a proliferative joint disease characterized by articular cartilage degeneration, osteophyte formation, subchondral bone sclerosis, and secondary induced synovitis [1]. Although numerous studies have revealed the contribution of genetic factors, growth factors and cytokines, mechanical stress, proteinase, or altered responses of chondrocytes in the progression of OA,

the pathogenesis of OA has not been fully understood.

High-mobility group box chromosomal protein (HMGB-1), previously called HMG-1 or amphoterin, named for its rapid mobility on electrophoresis gels, is a ubiquitous, approximately 27-kDa nonhistone protein with a highly conserved amino acid sequence identity between rodents and humans [2-4]. Nuclear HMGB-1 has been widely studied as a deoxyribonucleic acid (DNA)-binding protein. It participates in the maintenance of nucleosomal structure and stability and facilitates the binding of transcription factors to their cognate DNA sequences [5]. HMGB-1 also has func-

Received February 17, 2011; accepted July 29, 2011.

\*Corresponding author. Phone: +81-86-235-7273; Fax: +81-86-229-2797  
E-mail: knishida@md.okayama-u.ac.jp (K. Nishida)



tions in DNA transcription, recombination [6, 7], repair, cell replication, cell migration, and tumor growth [8, 9].

In contrast to its intranuclear role, HMGB-1 plays a critical role outside the cell as a proinflammatory cytokine mediating delayed endotoxin lethality as well as acute lung injury in mice [10, 11]. Moreover, high levels of HMGB-1 have been detected in the blood of patients with sepsis and in the synovial fluid of rheumatoid arthritis (RA) patients [12]. Proinflammatory mediators, such as tumor necrosis factor  $\alpha$  (TNF $\alpha$ ) and interleukin-1 $\beta$  (IL-1 $\beta$ ), dose-dependently induce the release of HMGB-1 from monocytes and macrophages [10]. Furthermore, once released, HMGB-1 activates an additional downstream cascade by stimulating monocytes to produce proinflammatory cytokines and chemokines [13].

The receptor for advanced glycation end products (RAGE) is a transmembrane protein that belongs to the immunoglobulin superfamily and is expressed in vascular smooth muscle cells, neurons, and certain phagocytes such as monocytes and macrophages [14]. Recently, the expression of RAGE has been reported in articular chondrocytes, synoviocytes, and RA synovial macrophages [15-17]. Membrane-associated HMGB-1 mediates cellular proliferation and growth by signaling through the receptor for RAGE [18].

Previous reports have suggested the HMGB-1 upregulation in OA cartilage and induction of inflammatory cytokines such as IL-6 or IL-8 [19]. In the current study, we investigated the expression and localization of nuclear and cytoplasmic HMGB-1 in normal human cartilage and OA cartilage. We further investigated the effect of HMGB-1 stimulation on TNF $\alpha$  and IL-1 $\beta$  production, as well as the effect of TNF $\alpha$  and IL-1 $\beta$  on HMGB-1 production by human OA chondrocytes. Our data strongly suggest the involvement of HMGB-1 in proinflammatory cytokines in cartilage destruction.

## Materials and Methods

**Production of HMGB-1-specific monoclonal antibody.** Rats were immunized with HMGB-1/HMGB-2 (Sigma, St. Louis, MO, USA) emulsified with Freund's complete adjuvant. A booster injection with incomplete adjuvant was administered to the rats 3 weeks later. After confirming the elevation of anti-

HMGB-1 antibody, we produced hybridomas as previously described [20]. The epitope recognized by each monoclonal antibody was determined by dot blotting, using synthetic overlapping peptides derived from a human HMGB-1 sequence 15 amino acids long. The clone (Nos. 10-22, subclass IgG2a) used for the experiments recognized the C-terminal sequence of the HMGB-1 molecule, DEDEEEE, as specific for HMGB-1 but not for HMGB-2.

### **Recombinant human HMGB-1 (rHMGB-1).**

rHMGB-1 was produced in Sf9 cells to obtain LPS-free HMGB-1. In brief, full-length human HMGB-1 DNA was amplified by PCR using Cap Site cDNA dT from human microvascular endothelial cells (Nippon Gene, Tokyo, Japan) and primers (forward 5'-GCA GAA TTC ATG GGC AAA GGA GAT CCT A-3', reverse 5'-CAT CTC GAG TCA TTA TTC ATC ATC ATC ATC-3'). The fragment was digested with EcoRI and XhoI and cloned into a pFastBacHTA (Invitrogen, Carlsbad, CA, USA) expression vector. The transfection of the Sf9 cells with the pFastBacHTA-HMGB-1 bacmid was performed according to the manufacturer's instructions (Bac-to-Bac Baculovirus Expression System, Invitrogen). The infected SF9 cell extract containing His-tagged HMGB-1 protein was applied to Ni-NTA agarose (Qiagen, Hilden, Germany) and incubated for 3 hours at room temperature. After extensive washing, rHMGB-1 was eluted with imidazole buffer. The rHMGB-1 was collected and dialyzed overnight at 4°C against PBS. Purified rHMGB-1 protein was identified by SDS-PAGE and Western blotting with anti-HMGB-1 mAb. The final HMGB-1 preparation contained LPS of less than 2.0 pg/ $\mu$ g protein.

**Human cartilage samples.** Thirty-one human OA cartilage samples were obtained at the time of total knee arthroplasty (TKA) surgery from 27 OA patients (aged 48 to 82 years; average, 70.7 years), who lacked a medical history of other inflammatory diseases. Normal cartilage was obtained from 4 patients with osteosarcoma (aged 9 to 29 years; average 15.5 years) who lacked any inflammatory diseases at the time of amputation surgery. Written informed consent was obtained from the patients or their parents.

**RNA isolation from OA cartilage.** OA cartilage samples from OA patients (n=4) and normal cartilage from osteosarcoma patients (n=4) were

divided in half; one half was immediately frozen in liquid nitrogen and stored at  $-180^{\circ}\text{C}$  until required for RNA isolation. At that point the frozen articular cartilage (10–40 mg wet weight) was milled with Micro Smash (Tomy Seiko Co, Tokyo, Japan) at 2 cycles of 1 min at 4,500 rpm and was suspended in 1 mL Isogen (Nippon Gene Co, Tokyo, Japan). Total RNA was isolated according to the manufacturer's protocol.

**cDNA synthesis and Quantitative Real-Time PCR.** First-strand cDNA was synthesized from 1  $\mu\text{g}$  total RNA using the ReverTra Ace- $\alpha$  according to the manufacturer's (Toyobo Co., Ltd., Osaka, Japan) instructions. cDNA (1.5  $\mu\text{L}$ ) was amplified by real-time PCR using Brilliant<sup>®</sup> II SYBR Green QPCR Master Mix (Stratagene, La Jolla, CA, USA). Quantitative PCR was performed on a 25- $\mu\text{L}$  samples. Mixtures were preincubated at  $95^{\circ}\text{C}$  for 10 min, followed by 40 cycles of PCR at  $95^{\circ}\text{C}$  for 30 sec and  $60^{\circ}\text{C}$  for 30 sec, and normalized to GAPDH. In every case, the cycle threshold ( $C_T$ ) taken for quantitation was in the linear portion of the amplification range. PCR primers were HMGB-1 sense, 5'-TAT GAA AAG AAG GCT GCG AAG-3'; and HMGB-1 antisense, 5'-CTG CGC TAG AAC CAA CTT ATT C-3'; GAPDH sense, 5'-CAT CAA GAA GGT GGT GAA GCA G-3'; and GAPDH; antisense, 5'-CTG CAA AGG TGG AGG AGT GG-3'. All PCRs were performed in triplicate using the Mx3000P quantitative PCR system (Stratagene). RNA levels are reported as fold changes compared with the control using the comparative quantitation analysis software available with the Mx3000P. Changes in expression (fold) for HMGB-1 were calculated as  $2^{-\Delta(\Delta C_T)}$ , where  $\Delta C_T = C_T(\text{target}) - C_T(\text{housekeeping})$ , and  $\Delta(\Delta C_T) = \Delta C_T(\text{treated}) - \Delta C_T(\text{control})$ . Reaction product purity was confirmed by examination of the melting curves for a single peak.

**Immunohistochemistry for HMGB-1 and RAGE.** Twenty-seven OA and 4 normal cartilage specimens were used in an immunohistochemical study for HMGB-1 and RAGE. The samples were immediately fixed in 4% paraformaldehyde in 0.1M phosphate-buffered saline (PBS), decalcified in 0.3M EDTA (pH 7.5) for 2–3 weeks, and embedded in paraffin. All sections were used for the histological and immunohistochemical studies.

The paraffin sections were soaked in xylene to be deparaffinized, then dehydrated in a graded alcohol

series (50–100%). Antigen retrieval was performed by autoclaving for 5 min at  $97^{\circ}\text{C}$ . After it was cooled, endogenous peroxidase activity was blocked by treatment with 0.3%  $\text{H}_2\text{O}_2$  in PBS at room temperature for 30 min. It was then incubated with either rat monoclonal anti-HMGB-1 antibody (10  $\mu\text{g}/\text{mL}$ ) or goat anti-RAGE polyclonal antibody (10  $\mu\text{g}/\text{mL}$ ) (Chemicon, Temecula, CA, USA) with PBS/bovine serum albumin (BSA) overnight at  $4^{\circ}\text{C}$ . After washing, the slides were incubated with biotinylated anti rat IgG antibody diluted 1:200 with PBS. After rinsing in PBS, the specimens were incubated with avidin-biotinylated enzyme complex (ABC) reagent (Vectastain Elite ABC Kit, Vector Laboratories, Burlingame, CA, USA), then washed with distilled water. For RAGE, a chemical reagent marketed as Histofine Simple Stain MAX PO (G) (Nichirei Biosciences, Tokyo, Japan) was applied as a secondary antibody at room temperature for 30 min. The reaction was visualized by diaminobenzidine, which turned brown, after which the samples were counterstained with hematoxylin.

**Quantitative analysis for HMGB-1 and RAGE-positive cells.** Immunoreactivity was evaluated by light microscopy. The chondrocytes with definite, diffusely stained cytoplasm or nuclei were regarded as positively stained. The populations of HMGB-1-positive, or RAGE-positive cells in the superficial, middle, and deep layers of OA cartilage, were quantified by counting the number of the cells within the 3 layers. Cell counts were performed in at least 3 fields, at  $\times 100$  magnification, and then averaged. Judgment was based on the consensus of at least 2 of the authors (C.T. and A.Y.) without reference to the patients' clinical information. The number of positive chondrocytes was divided by the total number of chondrocytes within all 3 layers to calculate the positive chondrocyte ratio. The marginal areas between each layer were avoided for cell counting to reduce inter-observer errors. All sections were also stained with Safranin O and observed by light microscopy. Histological classification of the severity of OA lesions was graded 1–6, using the OARSI cartilage OA histopathology grading system reported by Pritzker *et al.* [21].

**Chondrocyte isolation from OA cartilage.**

For the *in vitro* study, OA cartilage samples were obtained from another 6 sets of patients at TKA. The

ages of patients ranged from 62 to 88 years (mean  $\pm$  SEM  $72.1 \pm 8.2$  years). Chondrocytes were isolated by digestion of cartilage specimens in 0.1% chymotrypsin (Wako Pure Chemical Industries, Osaka, Japan) and 0.2% collagenase (Sigma, St. Louis, MO, USA) following the method of Bruckner *et al.* [22]. Chondrocytes were seeded in 6-well plates ( $5 \times 10^4$ /mL), cultured in 3mL Dulbecco's modified Eagle medium (Wako Pure Chemical Industries, Osaka, Japan) containing 10% fetal bovine serum, 100U/mL penicillin (Wako Pure Chemical Industries, Osaka, Japan), and 100  $\mu$ g/mL streptomycin (Wako Pure Chemical Industries, Osaka, Japan), and incubated in a 5% CO<sub>2</sub> humidified incubator at 37°C for 14 days before starting the experiments.

**Quantification of IL-1 $\beta$  and TNF $\alpha$  production by HMGB-1-stimulated chondrocytes.**

After exposure of the cells by recombinant human HMGB-1 (10, 100, and 1,000ng/mL) (Biological Industries, Kibbutz, Israel) for 6, 12, and 24h, the concentrations of IL-1 $\beta$  and TNF $\alpha$  in the supernatant were measured using a commercially available enzyme-linked immunosorbent assay (ELISA) kit (R&D Systems, Minneapolis, MN, USA), following the manufacturer's protocol.

**Quantitative Real-Time PCR for HMGB-1 mRNA in cytokine-stimulated chondrocytes.**

Recombinant human IL-1 $\beta$  and TNF $\alpha$  were purchased from R&D Systems. The cytokines were stored at -180°C and diluted in a culture medium immediately before being used. Total RNA was isolated from primary OA chondrocytes after treatment with IL-1 $\beta$  (10ng/mL) and TNF $\alpha$  (1ng/mL) for 0, 12, and 24h. HMGB-1 mRNA expression was analyzed by real-time PCR as previously described.

**Immunocytochemistry for HMGB-1 in cytokine-stimulated chondrocytes.**

Primary cultured OA chondrocytes were treated with IL-1 $\beta$  (10ng/mL) and TNF $\alpha$  (1ng/mL) for 48h, and the distribution of the HMGB-1 protein was investigated by immunocytochemistry. Cells were fixed in 4% paraformaldehyde for 10min, blocked with 1% BSA for 10min at room temperature, then incubated with an anti-HMGB-1 antibody (1  $\mu$ g/mL) for 30min at room temperature. A BSA solution without the primary antibody was used as a negative control. Alexa Fluor 488-conjugated antibody (Molecular Probes, Eugene, OR, USA) and Alexa-Fluor 594-conjugated phalloidin

(Molecular Probes), both incubated for 30min at room temperature, and Hoechst 33342 (ICN Biomedicals, Aurora, OH, USA), incubated for 5min at room temperature, were used for detection. Fluorescence images were captured using an inverted Leica DMRIII microscope (Leica, Bannockburn, IL, USA) equipped with epifluorescence filters and a charge-coupled device camera using Leica CW4000 software.

**Statistical analysis.** Statistical comparisons were made by Mann-Whitney *U* test using Stat-view software. All values are expressed as means  $\pm$  SEM. *P* values less than 0.05 were considered significant.

## Results

**Expression of HMGB-1 in OA cartilage.**

HMGB-1 was detected in normal and OA cartilage at both the mRNA and protein level. HMGB-1 mRNA expression was significantly higher in OA cartilage than in normal cartilage (Fig. 1).

**Expression and localization of HMGB-1 in OA cartilage.**

The protein expression of HMGB-1 was seen in all 27 OA cartilage samples (Fig. 2). HMGB-1-positive cell ratios relevant to the OA histopathology were 12.6% in Grade 1, 20.1% in Grade 2, 21.8% in Grade 3, and 34.2% in Grade 4 (Fig. 3A). In Grades 2, 3, and 4, HMGB-1-positive cell ratios were significantly higher than that in Grade 1. There was no significant difference between ratios in Grade 2 and 3. In Grade-4 OA, the HMGB-1-positive cell

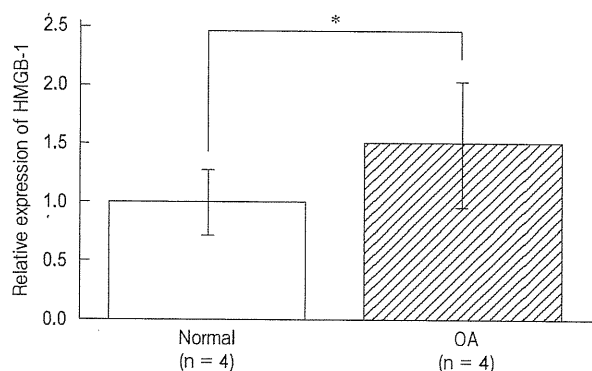
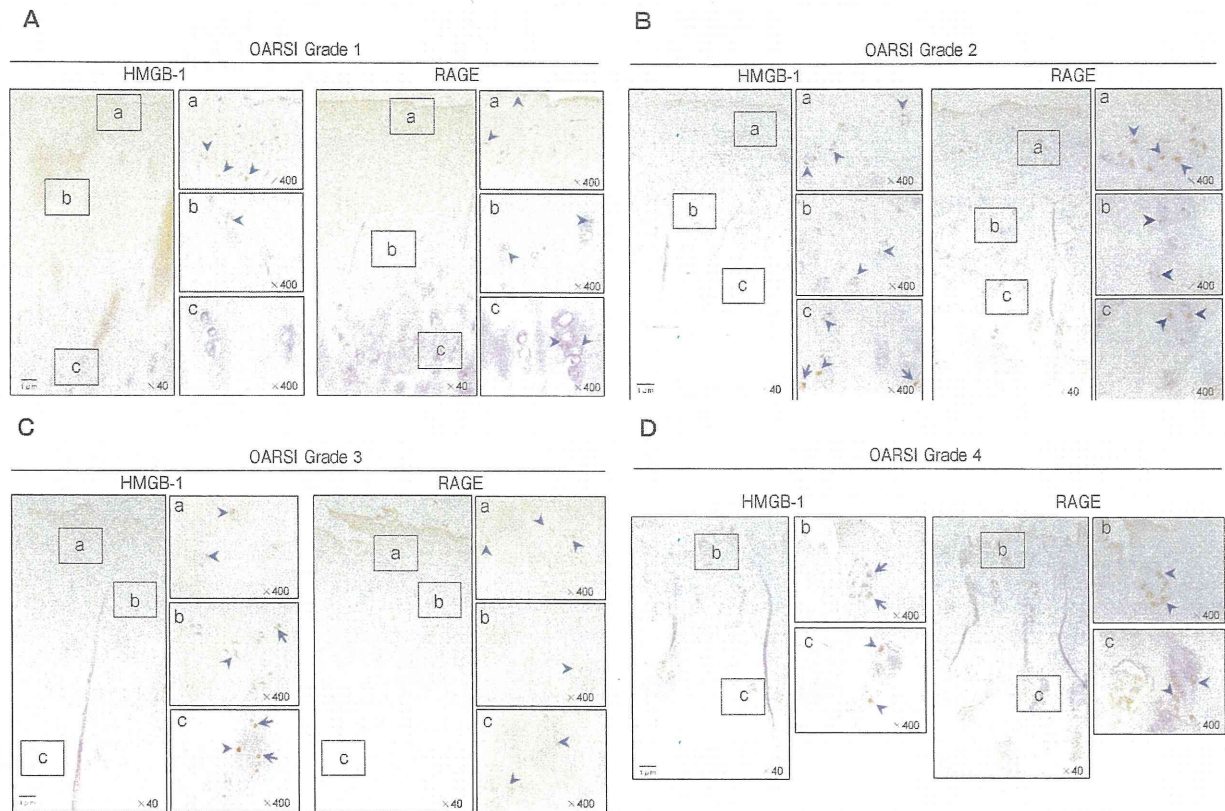


Fig. 1 Expression of HMGB-1 in OA cartilage. HMGB-1 expression in normal cartilage (n = 4) and OA cartilage (n = 4). HMGB-1 mRNA was significantly expressed. \**p* < 0.05 vs. normal (*p* = 0.043).



**Fig. 2** Immunohistochemistry for HMGB-1 and RAGE. Expression and localization of HMGB-1 and RAGE in OA cartilage in relation to the level of cartilage destruction. Twenty-seven OA and 4 normal cartilage specimens were used for the immunohistochemical study of HMGB-1 and RAGE. HMGB-1 was expressed in the nucleus. The cytoplasmic HMGB-1-positive cell rate tended to increase as the OARSI grade increased. RAGE was expressed in the cytoplasm, and the RAGE-positive cell ratio tended to be higher according to the OARSI grade, as with HMGB-1. Arrow heads indicate nuclear HMGB-1- and RAGE-positive cells, and arrows indicate cytoplasmic HMGB-1-positive cells. Inset a, b and c show the superficial, middle and deep layer, respectively.

ratio was significantly higher than those in Grade 2 or 3 (Fig. 3A). The cytoplasmic HMGB-1-positive cell rates were 1.4% in Grade 1, 2.3% in Grade 2, 11.1% in Grade 3, and 13.4% in Grade 4. In Grades 3 and 4, the cytoplasmic HMGB-1-positive cell ratios were significantly higher than those in Grade 1 and 2, respectively (Fig. 3A). There was no significant difference in ratios between Grade 1 and 2, or between Grade 3 and 4.

**Expression of RAGE in OA cartilage.** We also investigated RAGE expression in OA cartilage by immunohistochemical analysis. The RAGE-positive cell ratios relevant to OA histopathology were 20.4% in Grade 1, 36.6% in Grade 2, 37.3% in Grade 3, and 35.3% in Grade 4 (Fig. 3B). The ratios of RAGE

expression by chondrocytes in Grade 2, 3, and 4 were significantly higher than those in Grade 1 (Fig. 3B). There was no significant difference among ratio in Grades 2, 3, and 4. (Fig. 3B).

**Effect of proinflammatory cytokines on HMGB-1 expression and localization in OA chondrocytes.**

IL-1 $\beta$  (10 ng/mL) significantly up-regulated the expression of HMGB-1 mRNA up to 24h by OA chondrocytes (Fig. 4A); however, TNF $\alpha$  (1 ng/mL) up-regulation of HMGB-1 mRNA did not reach significance. The change in localization of HMGB-1 after treatment with IL-1 $\beta$  and TNF $\alpha$  was examined by immunocytochemistry. In the unstimulated group, HMGB-1 was localized in the nucleus (Fig. 4B). However, HMGB-1 was translocated from